The Structural Connectome of the Human Brain in Agenesis of the Corpus Callosum

Julia Owen[1], Yiou Li[1], Etay Ziv[1], Zoe Strominger[2], Jacquelyn Gold[2], Polina Bukshpun[2], Mari Wakahiro[2], Elliott Sherr[2], and Pratik Mukherjee[1]
[1]Radiology, UCSF, San Francisco, CA, United States, [2]Neurology, UCSF, San Francisco, CA, United States

Purpose: Adopting a network perspective, the structural connectome reveals the large-scale white matter connectivity of the human brain, yielding insights into cerebral organization otherwise inaccessible to researchers and clinicians[1,2,3,4]. Connectomics has great potential for elucidating abnormal connectivity in congenital brain malformations, especially axonal pathfinding disorders. Agenesis of the corpus callosum (AgCC) is one of the most common brain malformations. AgCC is considered a prototypical human disorder of axon guidance, one in which fibers that would normally have crossed the midline as part of the corpus callosum instead form Probst bundles, large white matter tracts that course anterior-posterior parallel to the interhemispheric fissure within each cerebral hemisphere[5]. In this exploratory study, the structural connectome of AgCC is mapped and compared to that of the normal human brain. Multiple levels of granularity of the AgCC connectome are investigated, including summary network metrics, modularity analysis, and network consistency measures, with comparison to the normal structural connectome after simulated removal of all callosal connections ("virtual callostomy").

Methods: Seven subjects with AgCC (4 male, 3 female; mean age 24.3±14.2, 5 right-handed) and 11 healthy volunteers (6 male, 5 female; mean age 24.9±9.1, 11 right-handed) were included in this study. All MR imaging was performed on a 3T EXCITE MR scanner (GE Healthcare, Waukesha, WI, USA) using an 8-channel head phased-array radio-frequency head coil. Whole-brain diffusion was performed with a multislice 2D single-shot spin-echo echo-planar sequence with 55 diffusion-encoding directions, a diffusion-weighting strength of b = 1000 s/mm^2; interleaved 1.8-mm axial sections; in-plane resolution of 1.8 x 1.8 mm. Motion correction and brain extraction were performed with FSL tools. FREESURFER was used to segment each subject's T1-weighted MRI [6]; 68 cortical labels and 14 subcortical labels were obtained as in [3,4]. The labels were registered to the diffusion space and were used as seed regions for probabilistic tractography using FSL's probtrackx2 [7] to create whole brain connectomes. A virtual callosotomy was performed on the controls by excluding any tracts that pass through the corpus callosum. The network measures (degree, betweenness, clustering coefficient, local efficiency, efficiency, cost, and characteristic path length) were computed using the Brain Connectivity Toolbox [8]. We applied the network measures to both the consensus networks and the individual networks in each group, which allowed for pair-wise statistics between the three groups. We used a non-parametric, resampling statistical procedure to assess group differences in the metrics. In addition, we also calculated metrics of consistency for the connection strengths and module assignments. We test for statistically significant different connection strengths in one module, the "structural core" of the cerebral cortex [2]; the p-values were corrected with a false discovery rate (FDR). A "virtual Probstotomy" is also performed on the AgCC subjects to assess the contribution of the Probst bundles to the AgCC connectome.

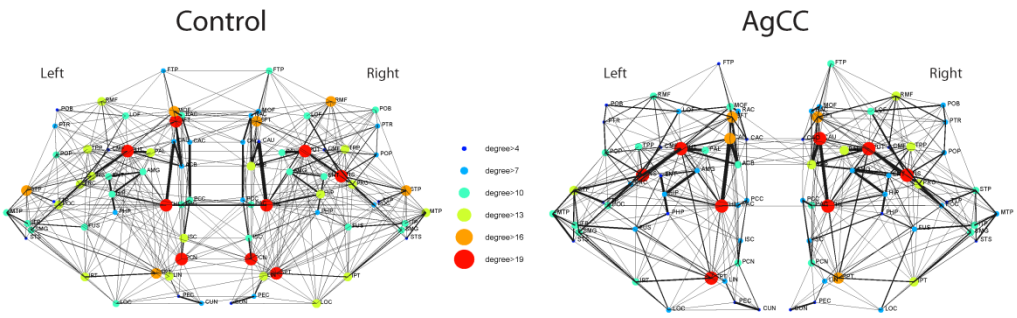

Figure 1: Consensus connectomes for the control and AgCC groups. The circles denote the 82 Freesurfer regions used as seeds for the tractography. The size and color of the circles indicate the degree of that region. An edge connecting two regions denotes a suprathreshold connection (keeping approx. the top 10% of connections).

Results: In Figure 1 we display the consensus connectomes for the control and AgCC groups to illustrate the differing network structure. Our quantitative investigations reveal four major findings. First, global connectivity is abnormally reduced in AgCC, but local connectivity is increased, Table 1. Second, the network topology of AgCC is more variable in both the connection strengths and the module assignments than that of the normal human connectome. Third, modularity analysis reveals that many of the tracts that comprise the structural core of the cerebral cortex have relatively weak connectivity in AgCC, especially the cingulate bundles bilaterally, Figure 2. Finally, virtual lesions of the Probst bundles in the AgCC connectome demonstrate that there is consistency across subjects in many of the connections generated by these ectopic white matter tracts, and that they are a mixture of cortical and subcortical fibers.

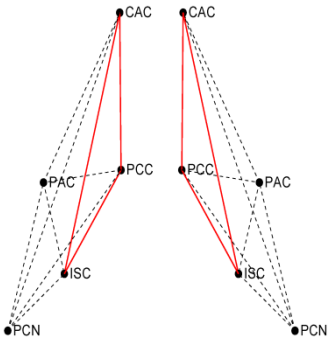

Figure 2: The backbone modules ("structural core") as identified in the control consensus connectome. The edges colored red were significantly weaker in the AgCC group compared to the controls at p<0.05, corrected for multiple comparisons using the false discovery rate.

Discussion and Conclusion: Together, these observations demonstrate that structural connectivity in AgCC, a classic axonal pathfinding disorder, is much more complex than is currently understood from prior studies using gross anatomical imaging or even diffusion tractography studies of specific fiber pathways [9,10]. The structural connectome of the acallosal brain reveals greatly altered connectivity in the AgCC brain that cannot be explained only by the absence of callosal fibers. Connectomics has great potential to more comprehensively elucidate the malformed human brain and advance our understanding of normal and abnormal brain development.

Network Metric	Control	Virtual Callosotomy	AgCC
Mean degree	17.7±2.2	14.9±1.5*	16.7±2.6
Cost	0.22±0.03	0.18±0.02*	0.21±0.03
Characteristic path length	1.98±0.09	2.36±0.09*	2.21±0.10*
Mean normalized betweenness	0.025±0.002	0.035±0.002*	0.031±0.002*
Global efficiency	0.57±0.03	0.51±0.02*	0.53±0.03*
Mean local efficiency	0.79±0.01	0.81±0.01*	0.83±0.03*
Mean clustering coefficient	0.59±0.02	0.64±0.02*	0.67±0.04*

Table 1: Network metrics applied to individual connectomes, * denotes statistically different than controls (p<0.05)

References: [1] Sporns, O. (2005), [2] Hagmann, P. (2008), [3] van de Heuvel, M.P. (2011), [4] Li, L. (2011), [5] Paul (2007), [6] Desikan, R.S (2006) , [7] Behrens, T.E.J (2003), [8] Rubinov (2010), [9] Tovar-Moll, F. (2007), [10] Wahl, M. (2009)